Publié par :
Published by:
Publicación de la:

Faculté des sciences de l'administration
2325, rue de la Terrasse
Pavillon Palasis-Prince, Université Laval
Québec (Québec) Canada G1V 0A6
Tél. Ph. Tel. : (418) 656-3644
Télec. Fax : (418) 656-7047

Disponible sur Internet :
Available on Internet
Disponible por Internet :

http://www4.fsa.ulaval.ca/la-recherche/publications/documents-de-travail/

DOCUMENT DE TRAVAIL 2018-016

Optimizing Drinking Water
Distribution System Operations

Bruno S. VIEIRA
Sérgio F. MAYERLE
Lucila M. S. CAMPOS
Leandro C. COELHO

Document de travail également publié par le Centre interuniversitaire de recherche sur les réseaux d'entreprise, la logistique et le transport, sous le numéro CIRRELT-2018-29

Juin 2018

Dépôt legal – Bibliothèque et Archives nationales du Québec, 2018
Bibliothèque et Archives Canada, 2018

ISBN 978-2-89524-473-8 (PDF)

Optimizing Drinking Water Distribution System Operations

Bruno S. Vieira[1*], **Sérgio F. Mayerle**[2], **Lucila M. S. Campos**[2], **Leandro C. Coelho**[3]

[1] Department of Industrial Engineering, Instituto Federal de Santa Catarina, Brazil
[2] Department of Industrial Engineering, Universidade Federal de Santa Catarina, Brazil
[3] Interuniversity Research Centre on Enterprise Networks, Logistics and Transportation (CIRRELT) and Department of Operations and Decision Systems, 2325, rue de la Terrasse, Université Laval, Québec, Canada, G1V 0A6

**Corresponding author: bruno.vieira@ifsc.edu.br*

ABSTRACT

Due to the fast pace of urbanization, governments and water supply service providers have struggled to manage the services and the expansion of investments. The operation of Water Distribution System (WDS) is often complex, especially when considering the changes in tariffs throughout the day. The cost of energy in these systems can reach 30% of total operating costs and its careful management can represent increased efficiency. The optimization of WDS scheduling operation appears as an effective method to reduce operating costs while ensuring a good service level to the population. In this paper we propose a new linear relaxation for a non-linear integer programming formulation for WDS in order to optimize its operation costs. We test our method on three benchmark instances from the literature improving all solutions from the competing algorithms. We also apply it to a larger new instance obtained from the WDS from the city of Florianópolis, southern Brazil, significantly outperforming the current solution employed by the utility provider. This study makes four main contributions. First, our formulation includes new aspects related to the capacity of storage tanks that were not considered before, which yields a more realistic representation of the physics of water and tanks. Second, our linearization technique includes a variable number of breakpoints, resulting in significantly fewer binary variables for a given error level. Third, our relaxation reduces the search of the space solutions. Lastly, we provide a new real-life instance and improve the solutions for three available benchmark instances.

Keywords: Water distribution system, operations, mathematical programming, optimization.

Acknowledgments: This project was partly funded by the Natural Sciences and Engineering Research Council of Canada (NSERC) under grant 2014-05764, and by the Brazilian National Council for Scientific and Technological Development (CNPq). This support is greatly acknowledged.

1 Introduction

Distribution of drinking water is a key service offered to society. By 2030, water demand will exceed the supply capacity by 40% by current resource management practices [1]. With increased urbanization, governments cannot improve their infrastructure at the same pace, but changing the way they operate it can yield significant improvements, which might be critical especially in developing areas [5].

One of the most important costs in Water Distribution Systems (WDS) is that related to the electricity used to pump water. Indeed, about 2% to 3% of the global energy consumption is used in WDS [15], which accounts for up to 30% of total WDS operating costs [16]. It is then crucial for water utility providers to develop efficient water distribution plans to reduce their costs.

However, WDS operation is quite complex. Pumps must be turned on and off to guarantee a flow of water throughout the system to satisfy all demand points. Conversely, operating pumps increase the pressure on the pipes. If the pressure is too low, water will not reach the highest points of the network and will make the system prone to intrusion; if pressure is too high, leaks will occur, and more energy than the necessary will have been used, increasing costs. In addition to different energy tariffs throughout the day, the system operation is subject to strongly non-linear hydraulic flow resistance, called head loss, and several points throughout the network are subject to strict pressure bounds. Moreover, the system is composed of other infrastructure, some of which can have their status modified throughout the day. These are the valves and tanks. Valves act on pipes by only allowing flow in one direction, and tanks are used as an inventory of water. When pressure is high and demand is low, this inventory increases and the tanks accumulate water. When demand increases and the surrounding pressure decreases, gravity flows the water from the tanks to the network of pipes. The combination of these factors makes the optimization of even very small networks difficult [14]. Optimization has been used to help on expansion plans [9, 24], determining pipe size [2, 10], and on daily operations [3, 13, 18, 19, 26, 27], the focus of this paper, as described next.

Ghaddar et al. [13] used a Lagrangian decomposition applied to a non-linear formulation of pumping plan and obtained an optimal solution for a schematic version of the WDS of the Richmond region, UK, which consists of seven pumps, 47 nodes and 44 pipes [25]. Their algorithm took about two hours of computing time. The same system, with different tariffs, was solved by Giacomello et al. [14], who used linear programming coupled with a local search method. The solution was presented within seconds, but did not guarantee optimality. Moreover, the comparison to the original cost structure

was not performed.

Relaxations of non-linear programming formulations have been used to drive search algorithms. Geiβler et al. [12] proposed an adaptive refinement of mixed-integer programming relaxations for a gas network whose operation is similar to that of water networks. Their algorithm computes the maximum error incurred by the relaxation and refines the constraints associated with them. This method was shown to outperform commercial mixed-integer non-linear programming solvers on three instances of their problem, that contained up to 452 pipes, six compressor stations (equivalent to the pumps in water systems) and 34 valves.

López-Ibáñez et al. [17] developed an ant colony optimization metaheuristic to explicitly define the times at which pumps must be turned on and off. The authors solved two variants of the Richmond WDS, the biggest one containing 872 nodes (including six tanks and one water source), 957 arcs, seven pumps and 21 valves. A genetic algorithm was proposed by Marchi et al. [19] to define control rules used to optimize a test network described in Van Zyl et al. [26], which consists of one valve and two consumption nodes, supplied by three pumps and two water reservoirs, for a total of 16 nodes and 18 arcs.

Mathematical programming has recently gained momentum in solving WDS, which can be well described by a mixed-integer non-linear programming (MINLP) formulation. D'Ambrosio et al. [7] describe some algorithmic paradigms widely applied to MINLPs and show how they have been applied to water network optimization. The authors highlight that mixed-integer linear programming (MILP) approximations have been used to solve WDS problems, especially those exploiting piecewise approximations and relaxations. The interested reader is referred to Rovatti et al. [22] and to Geiβler et al. [11]. An overview of the mathematical techniques used in WDS can be found in D'Ambrosio et al. [7], while a more general overview of the main methods, results and networks studied in the literature can be found at Coelho and Andrade-Campos [4].

Besides financial gains, determining the best pumping plan in order to satisfy all constraints and minimizing pumping costs can have several side benefits. An efficient plan can avoid the unnecessary use of resources and minimize the ecological impact of pollution and emissions of greenhouse gases [13]. Moreover, high pressure is known to be a major cause of leakage [28], and thus, of wasting treated water, which is not environmental friendly.

In this paper we propose a new linear relaxation for a MINLP formulation for WDS in order to optimize its operation costs. The relaxation yields approximations, and we develop a new method

which iteratively refines them, based on Geiβler et al. [12]. In our method, we initially stipulate a maximum error for each piecewise relaxation, defining each breakpoint in a way not yet explored in the literature. The relaxations are computed such that they reduce the solution space, and the breakpoints are defined such that for each pipe, each piecewise relaxation stretch has the same maximum error, which is monotonically decreasing. Aiming at the feasibility of the solution to the original problem, we developed a procedure to systematically correct linearization-induced errors. If the procedure does not lead to a feasible or satisfactory result, the maximum tolerated error is tightened and computed, and the linearization and optimization procedures are iterated once more.

We test our algorithm on three benchmark instances from the literature, besides applying it to a new instance obtained from the WDS from the city of Florianópolis, southern Brazil. Our results improve all the solutions from the literature and we provide solutions that are significantly better than the current practice employed by the utility provider in Florianópolis.

This paper has four main contributions. First, our MINLP formulation includes new aspects related to the tanks capacity that were not considered before, which yields a more realistic representation of the physics of water and tanks. Second, our linearization of the non-linearities includes a variable number of breakpoints, resulting in significantly fewer binary variables for a given error level. Third, our algorithm has always been able to convert relaxed solutions into feasible ones, for all benchmark instances studied. Finally, we improve the solutions of all available benchmarks and provide a new real-life instance, larger than any of those available in the literature.

The remainder of this paper is organized as follows. In Section 2 we provide a formal description of the problem along with mathematical models, including the non-linear and linear formulations of the problem. Our main technical and algorithmic developments are presented in Section 3. We describe the computational experiments used to validate our model on benchmark instances from the literature in Section 4, where we also describe a new WDS made available for the community. Our conclusions follow in Section 5.

2 Problem description and mathematical formulations

A WDS can be modeled on a graph consisting of arcs and nodes. Nodes represent water sources, tanks and junctions, which may have a demand. Let $\mathcal{A}$ be the set of all nodes, partitioned into the set $\mathcal{R}$ of water sources, the set $\mathcal{K}$ of tanks and the set $\mathcal{J}$ of junctions. Arcs on the graph represent the pipes

of the system, identified by the set $\mathcal{N}$. To each pipe with endpoints i and j, there is an associated maximum flow Q_{ij} (in liters per second), a length L_{ij} (in meters), a radius R_{ij} (in meters), and a roughness coefficient K_{ij}. Let $\mathcal{P} \subset \mathcal{N}$ be the subset of pipes containing pumps and $\mathcal{V} \subset \mathcal{N}$ be the subset of pipes containing valves, such that $\mathcal{P} \cap \mathcal{V} = \emptyset$.

The problem is defined over a finite horizon in the set $\mathcal{T}$, with $|\mathcal{T}| = H$ and $\triangle T$ being the length of each time period. When a pump is operating, an electricity cost is due. Let C_{ijt} be the cost for pump $(i, j) \in \mathcal{P}$ at time period $t \in \mathcal{T}$, measured in monetary units per kW.

For each node i, its elevation E_i (in meters) is known, its minimum and maximum pressure bounds are given by P_i^L and P_i^U (in meters), and the demand of each junction j in period t is given by D_{jt} (in liters per second). Water source r is associated with its pressure per period P_{rt} (in meters). A tank i is associated with a surface area A_i (in squared meters) and a capacity B_i (in meters). Finally, let γ represent the specific weight of water (N/m^3).

We now present two models for the operations of a WDS. In Section 2.1 we present a MINLP formulation, and in Section 2.2 a MILP formulation using piecewise linear relaxations as an approximation for the MINLP model. Section 2.3 describes some simplifications and tightening we have developed for our models.

2.1 Mixed-integer non-linear programming formulation

The variables of the model as are follows. Let q_{ijt} represent the flow through pipe (i, j) in period t, and h_{ijt} be the head loss in pipe (i, j) in period t. Let binary variables s_{ijt} be equal to one if pump, valve or outflow of tank (i, j) is active in period t, and binary variables f_{it} be equal to one if the level of water in the tank i is at the limit of its capacity at the beginning of period t. Let the pressure on node i in period t be represented by variable p_{it} and its auxiliary variable p'_{it}. Finally, let η_{ij} represent the efficiency of pump installed on pipe (i, j), which is a flow function. The problem (P) can then be formulated as follows:

$$(P) \quad min \sum_{t \in \mathcal{T}} \sum_{(i,j) \in \mathcal{P}} \frac{\gamma q_{ijt} h_{ijt} C_{ijt}}{10^6 \eta_{ij}} \tag{1}$$

subject to

$$q_{ijt} \leq Q_{ij} \quad (i,j) \in \mathcal{N} \backslash (\mathcal{P} \cup \mathcal{V} \cup (i \in \mathcal{K})), t \in \mathcal{T} \tag{2}$$

$$q_{ijt} \leq s_{ijt} Q_{ij} \quad (i,j) \in \mathcal{P} \cup \mathcal{V} \cup (i \in \mathcal{K}), t \in \mathcal{T} \tag{3}$$

$$\sum_{i \in \mathcal{A}} q_{ijt} - \sum_{k \in \mathcal{A}} q_{jkt} = D_{jt} \quad j \in \mathcal{J}, t \in \mathcal{T} \tag{4}$$

$$q_{ijt}((p_{it} + E_i) - (p_{j,t} + E_j) - h_{ijt}) = 0 \quad (i,j) \in \mathcal{N} \backslash (\mathcal{P} \cup \mathcal{V} \cup (i \in \mathcal{K})), t \in \mathcal{T} \tag{5}$$

$$(p_{it} + E_i) - (p_{jt} + E_j) - h_{ijt} \leq 0 \quad (i,j) \in \mathcal{N} \backslash \mathcal{P}, t \in \mathcal{T} \tag{6}$$

$$s_{ijt}((p_{it} + E_i) - (p_{jt} + E_j) + h_{ijt}) = 0 \quad (i,j) \in \mathcal{P}, t \in \mathcal{T} \tag{7}$$

$$s_{ijt}((p_{it} + E_i) - (p_{jt} + E_j) - h_{ijt}) = 0 \quad (i,j) \in \mathcal{V} \cup i \in \mathcal{K}, t \in \mathcal{T} \tag{8}$$

$$h_{ijt} = \frac{10.64 \frac{q_{ij,t}}{1000}^{1.852} L_{ij}}{K_{ij}^{1.852} (2R_{ij})^{4.87}} \quad (i,j) \in \mathcal{N} \backslash \mathcal{P}, t \in \mathcal{T} \tag{9}$$

$$h_{ijt} = f_{ij}(q_{ijt}) \quad (i,j) \in \mathcal{P}, t \in \mathcal{T} \tag{10}$$

$$\eta_{ij} = g_{ij}(q_{ijt}) \quad (i,j) \in \mathcal{P}, t \in \mathcal{T} \tag{11}$$

$$P_i^L \leq p_{it} \leq P_i^U \quad i \in \mathcal{A} \backslash \mathcal{R}, t \in \mathcal{T} \tag{12}$$

$$p_{it} = P_{rt} \quad i \in \mathcal{R}, r \in \mathcal{R}, t \in \mathcal{T} \tag{13}$$

$$p'_{jt} = p_{j,t-1} + 3.6 \frac{\sum_{i \in \mathcal{A}} q_{ij,t-1} - \sum_{k \in \mathcal{A}} q_{jk,t-1}}{A_j} \quad j \in \mathcal{K}, t \in \mathcal{T} \backslash (1), \tag{14}$$

$$p'_{j,1} \leq p_{jt} + 3.6 \frac{\sum_{i \in \mathcal{A}} q_{ijt} - \sum_{k \in \mathcal{A}} q_{jkt}}{A_j} \quad j \in \mathcal{K}, t \in \mathcal{T} \tag{15}$$

$$p'_{jt} \leq P_j^U + f_{jt} B \quad j \in \mathcal{K}, t \in \mathcal{T} \tag{16}$$

$$p'_{jt} \geq P_j^U f_{jt} \quad j \in \mathcal{K}, t \in \mathcal{T} \tag{17}$$

$$s_{ijt} \geq 1 - f_{it} \quad i \in \mathcal{K}, j \in \mathcal{J}, t \in \mathcal{T} \tag{18}$$

$$f_{jt} P_j^U = f_{jt} p_{jt} \quad j \in \mathcal{K}, t \in \mathcal{T} \tag{19}$$

$$p_{jt}(1 - f_{jt}) = p'_{jt}(1 - f_{jt}) \quad j \in \mathcal{K}, t \in \mathcal{T} \tag{20}$$

$$q_{ijt} > 0, s_{ijt} \in \{0,1\} \quad (i,j) \in \mathcal{N}, t \in \mathcal{T}. \tag{21}$$

The objective function (1) minimizes the total power consumption. Constraints (2) impose an upper bound on the flow on each pipe, while constraints (3) ensure that the flow on a pipe occurs only if the corresponding pump, valve or pipe leading to the tank is active. Constraints (4) enforce water conservation, while constraints (5)–(9) model energy conservation based on the hydraulic properties of the system. Equations (5) ensure that the flow can only happen in one direction at a time, respecting energy conservation laws. Inequalities (6) guarantee that when the flow is zero from j to i and from

i to j, energy conservation is satisfied. Constraints (7) ensure that the flow through the pump is in accordance with the energy conservation and (8) ensure the conservation of energy for pipes with valves and tank outputs. Constraints (9) represent the Hazen-Williams (HW) head loss equation. Constraints (10) and (11) represent the pump characteristic and yield curves, respectively, and both depend on the flow. Constraints (12) represent the minimum and maximum pressure for nodes without water sources, which in turn, have their pressure bounded by (13). Constraints (14) correspond to mass balance equations and (15) impose that the level of the tanks at the end of the horizon to be at least that of the initial period. Constraints (16) and (17) allow the auxiliary pressure variable to exceed its maximum value when the tank is full. In this case, constraints (18) allow disjoining arcs that flow into the tank, while (3) and (6) enforce their connection when the water is flowing from the tank. Moreover, if the tank is full, i.e., variable f_{it} is equal to 1, constraints (19) require the tank pressure to be at its upper limit. On the other hand, when f_{it} equals zero, constraints (20) impose the auxiliary pressure variable p' to be equal to the original pressure variable p. These tank-related restrictions allow us to consider the conditions when the tank is full. In this situation, the system usually operates in a very particular condition, which must be considered in the search for optimal solutions. We did not find other studies that consider this feature. Finally, constraints (21) define the domain and nature of the variables.

2.2 Mixed-integer linear programming formulation

This formulation is based on MINLP model (P) just presented, but relaxes and approximates its non-linearities. These are depicted in Figure 1. The objective function (1) will be approximated using a piecewise linear function as shown in Figure 1a. Pump characteristic curves representing the pair flow-pressure of constraints (10) will be bounded as in Figure 1b, and the HW conditions (constraints (9)) will be relaxed and bounded via a piecewise linear function as in Figure 1c. The use of piecewise relaxations instead of an approximation, as used by Geiβler et al. [11] and Geiβler et al. [12], for pump characteristics and the HW curves are chosen because they offer several advantages. First, solutions to the original problem are feasible in the relaxed one, allowing us to exploit initial solutions and warm starts in our MILP formulation. Second, if we can prove that the relaxed problem is infeasible, the original problem will also be [12], which is not the case in the use of approximations. Finally, since the objective function of the relaxed problem is an underestimation of (1), all solutions of the MILP are valid lower bounds for the original problem.

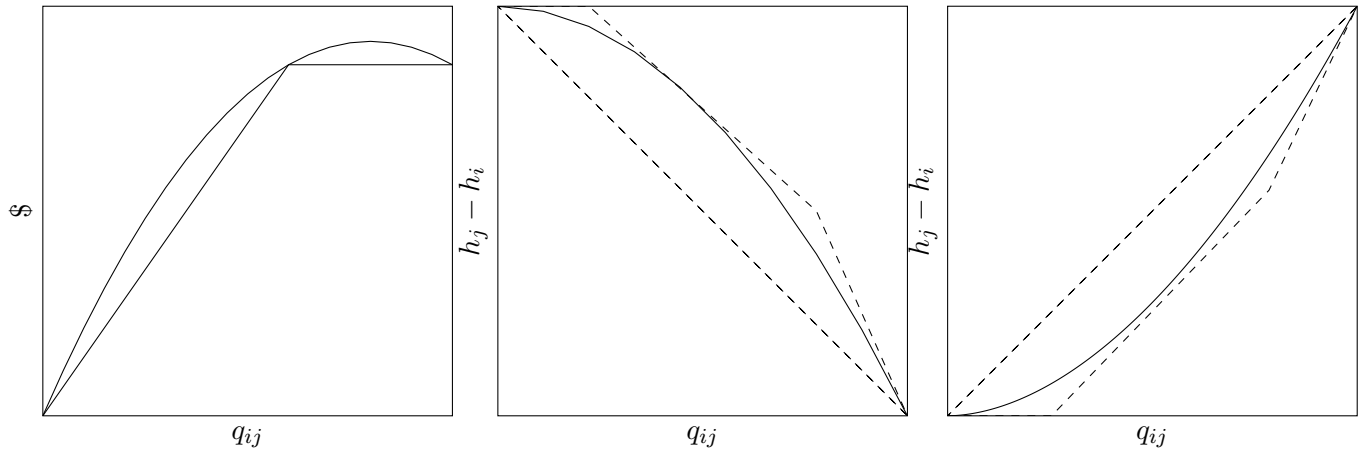

(a) Objective function curve **(b)** Characteristic pump curve **(c)** Hazen-Williams curve

Figure 1: Piecewise linear relaxation and approximation of non-linearities

In order to develop the linear version of the model, let us define additional sets, parameters and variables. Let $\mathcal{O}$ be the set of breakpoints of the HW function and pump curves, $\mathcal{G}$ be the set of straight lines coefficients of all segments that define bounds for the relaxations, partitioned into $\mathcal{G}^U$ and $\mathcal{G}^L$ being the subsets of straight lines coefficients that define upper and lower bounds, respectively. New parameters are defined as follows. Let Q_{oij}^{HW} be the flow points $o \in \mathcal{O}$ where the linearized curves will necessarily have the same pressure values of the original HW curve (i, j). Hence, let $H_{oij}^{HW}(Q_{oij}^{HW})$ be the pressure at corresponding points of Q_{oij}^{HW} value, where:

$$H_{oij}^{HW}(Q_{oij}^{HW}) = \begin{cases} \frac{10.641 L_{ij} \frac{{Q_{oij}^{HW}}^{1.852}}{1000}}{C_{ij}^{1.852} D_{ij}^{4.87}} & \text{if } Q_{oij}^{HW} > 0 \\ -\frac{10.641 L_{ij} \frac{{-Q_{oij}^{HW}}^{1.852}}{1000}}{C_{ij}^{1.852} D_{ij}^{4.87}} & \text{if } Q_{oij}^{HW} < 0. \end{cases} \tag{22}$$

Also, let Q_{oij}^{P} be the flow points $o \in \mathcal{O}$ where the linearized curves will necessarily have the same pressure values of the original pump curve and the same cost values of the original objective function, for the pipe (i, j). In this case, let $H_{oij}^{P}(Q_{o,ij}^{P})$ be the pressure corresponding points of Q_{oij}^{P} value in the original curve. Finally, let $Z_{oij}^{P}(Q_{o,ij}^{P})$ be the cost corresponding points of Q_{nij}^{P} value in the original curve, where:

$$Z_{oij}^{P}(Q_{oij}^{P}) = \sum_{t=1}^{\mathcal{T}} \sum_{(ij)\in\mathcal{P}} \frac{\gamma C_{ijt} Q_{oij}^{P} H_{oij}^{P}}{10^6 \eta_{ij}}. \tag{23}$$

The following variables must also be defined. Let λ_{oijt} be equal to 1 if the piecewise segment o of pipe

(i,j) is active in period t, and 0 otherwise. This is used for approximating the objective function. We develop our piecewise approximation of the objective function using the convex-combination method [8], which is based on the principle that it is possible to compute the function at a given point by the convex combination of neighboring nodes. Thus, the objective function (1) must be replaced by (24)–(28):

$$min \sum_{t\in\mathcal{T}} \sum_{(i,j)\in\mathcal{P}} \sum_{o\in\mathcal{O}} \lambda_{oijt} Z^{\mathcal{P}}_{oij} \tag{24}$$

$$q_{ijt} = \sum_{o\in\mathcal{O}} \lambda_{oijt} Q^{P}_{oij} \quad (i,j)\in\mathcal{P}, t\in\mathcal{T} \tag{25}$$

$$\sum_{o\in\mathcal{O}} \lambda_{oijt} = 1 \quad (i,j)\in\mathcal{P}, t\in\mathcal{T} \tag{26}$$

$$\lambda_{oijt} \leq b_{o-1,ijt} + b_{oijt} \quad (i,j)\in\mathcal{P}, o=1,\ldots,|\mathcal{O}|-1, t\in\mathcal{T} \tag{27}$$

$$\lambda_{oijt} \geq 0 \quad (i,j)\in\mathcal{P}, o=1,\ldots,|\mathcal{O}|-1, t\in\mathcal{T}. \tag{28}$$

In turn, the HW equations (9) and the pump flow-pressure curves (10) have been relaxed and each convex portion has been limited by four straight inequalities, forming an envelope around the original function. Each envelope is activated by the value of a corresponding binary variable. It is noteworthy that the outside of the concavity could be bounded by countless straight lines, without the need of extra binary variables. Thus, these constraints must be changed by inequalities with the generic form shown in (29) and (30):

$$b_{o,ij,t}(A_{goij} q_{ij,t} + B_{goij}) \geq b_{o,ij,t} h_{ij,t} \quad (i,j)\in\mathcal{N}, o=1,\ldots,|\mathcal{O}|-1, g\in\mathcal{G}^{U}, t\in\mathcal{T} \tag{29}$$

$$b_{o,ij,t}(A_{goij} q_{ijt} + B_{goij}) \leq b_{oijt} h_{ij,t} \quad (i,j)\in\mathcal{N}, o=1,\ldots,|\mathcal{O}|-1, g\in\mathcal{G}^{L}, t\in\mathcal{T}, \tag{30}$$

where A_{goij} and B_{goij} are the straight lines coefficients that limit the original curve. Inequalities (29) and (30) are non-linear, but linearizing them is trivial. The same method was used to linearize (7), (8), (19) and (20). Furthermore, one of the envelopes of each pipe must necessarily be activated, as indicated by constraints (31):

$$\sum_{o=1}^{|\mathcal{O}|-1} b_{o,ij,t} = 1 \quad (i,j)\in\mathcal{N}, t\in\mathcal{T}. \tag{31}$$

Finally, energy conservation equations (5) must be replaced by (32):

$$(p_{i,t} + E_i) - (p_{j,t} + E_j) - h_{ij,t} = 0 \quad (i,j) \in \mathcal{N} \backslash (\mathcal{P} \cup \mathcal{V} \cup (i \in \mathcal{K})), t \in \mathcal{T}. \tag{32}$$

Note that once the equation (9) is linearized, h_{ijt} may assume positive and negative values. Equations (11) are no longer necessary since the efficiency functions are embedded in the objective function. Finally, the domain of the q variables in (21) must now allow negative flows.

2.3 Model refinement

In this section we describe some simplifications and valid inequalities we have developed for our models. First, we simplify it by what we call *notable flows*. For arcs that follow a tank towards the end of a network without any loops, the flow can be predetermined as a function of the demands. Figure 2 shows a small part of a network, in which the flow of arcs (6,4), (6,5), (7,6) and (8,7) can be pre calculated as follows, assuming Q^{Pre}_{ijt} is the predetermined flow on arc (i,j) in period t:

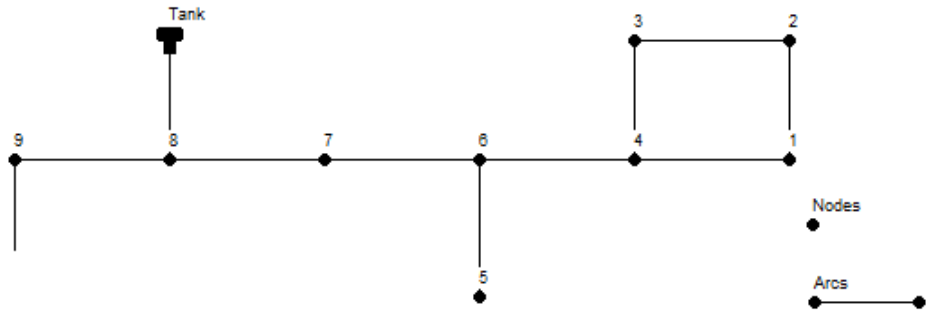

Figure 2: Part of a network – notable flows

$Q^{Pre}_{6,4,t} = D_{4,t} + D_{3,t} + D_{2,t} + D_{1,t}$
$Q^{Pre}_{6,5,t} = D_{5,t}$
$Q^{Pre}_{7,6,t} = D_{6,t} + Q^{Pre}_{6,5,t} + Q^{Pre}_{6,4,t}$
$Q^{Pre}_{8,7,t} = D_{7,t} + Q^{Pre}_{7,6,t}$

Moreover, in some cases some *shortcuts* can be derived. These appear when the maximum head loss on a pipe has a negligible value. This strategy was used, for example, in Geiβler et al. [12]. We can then simplify (8) and (32) as follows:

$$(p_{i,t} + E_i) - (p_{j,t} + E_j) = 0 \quad (i,j) \in \mathcal{N} \backslash (\mathcal{P} \cup \mathcal{V} \cup (i \in \mathcal{K})), t \in \mathcal{T} \tag{33}$$

$$s_{ij,t}((p_{i,t} + E_i) - (p_{j,t} + E_j)) = 0 \quad (i,j) \in \mathcal{V} \cup (i \in \mathcal{K}), t \in \mathcal{T}. \tag{34}$$

Also, it is common practice by utility providers to limit the number of times a pump is turned on and off. This can be incorporated in our models by using a new binary variable m_{ijt} equal to 1 if pump (i,j) is switched on in period t. Letting M be the maximum number of switches allowed per pump, we can add the following constraints to the model:

$$m_{ijt} + s_{ij,t-1} \geq s_{ij,t} \quad (i,j) \in \mathcal{P}, t \in \mathcal{T} \tag{35}$$

$$\sum_{t \in \mathcal{T}} m_{ijt} \leq M \quad (i,j) \in \mathcal{P} \tag{36}$$

$$m_{ijt} \in \{0,1\}. \tag{37}$$

Moreover, it is known that valid inequalities can accelerate the resolution of MILP models [6]. We now introduce some classes of valid inequalities.

As is typical in this literature and to ensure sustainable operations over time, the volume of water at the tanks at the end of the planning horizon must be at least equal to that at the initial period. Given this characteristic, we can determine a lower bound on the number of switches performed. This is achieved by defining the set $\mathcal{P}_r$ as that of pumps drawing water from sources. The constraint is then:

$$\sum_{k \in \mathcal{K}} A_k(p_{k1} - p_{kt}) + 3.6 \sum_{t'=t}^{H} D_{it'} \leq 3.6 \sum_{(i,j) \in \mathcal{P}_r} \sum_{t'=t}^{H} s_{ijt'} Q_{ij} \quad t \in \mathcal{T}. \tag{38}$$

We have also observed in real networks that parallel valves can direct the flow of water through a pump (or not in case these valves are closed). In any way, the water either flows through the pump or loops it completely, but never via both ways. When such a structure is present, we can add the following cut:

$$S_{via\,pump} + S_{not\,via\,pump} \leq 1. \tag{39}$$

Finally, when two identical pumps are installed in parallel, the number of combinations for their activation can be reduced via lexicographic ordering:

$$s_{pump_1,t} \leq s_{pump_2,t} \quad t \in \mathcal{T}, \text{for parallel pumps 1 and 2.} \tag{40}$$

3 Solution algorithm

In this section we describe the ideas used to simplify the solution of the mathematical model just presented and to ensure a feasible and good solution is obtained. In Section 3.1 we describe how we define breakpoints to limit the maximum tolerated error and to refine them at each iteration. Then, in Section 3.2 we develop an algorithm to derive feasible solutions from the relaxations obtained from the first phase. In general, our algorithm works in four main steeps, as follows:

1. definition of a maximum tolerated error;
2. linearization of the mathematical model using binary variables to enforce the maximum error, yielding a model which is piecewise linear;
3. resolution of the linear model (by a commercial solver);
4. computation of the real costs of the solution from step 3 (using a water distribution system simulation solver).

3.1 Definition of the breakpoints

In the previous model, the efficiency curves of the pumps of the system and the HW head loss curves are non-linear and complicating in terms of solving the problem. In Geiβler et al. [12], the vertical distance h_{ijt} was used as the maximum error. We better estimate and bound this error by encapsulating each curve by a set of straight lines, corresponding to a small portion of the curve defined for a pair (q_{ijt}, h_{ijt}). Hence, for each pump we can define and compute the maximum horizontal distance q_{ijt} for each point h_{ijt}. Moreover, for each arc we can define and compute the maximum vertical distance h_{ijt} for each point q_{ijt}. These are depicted in Figures 3a and 3b.

Note that these error values can be established a priori for each arc. Each linearized area is then defined by its minimum and maximum flow points, determining the breakpoints of the linearization. The maximum error can be refined by adding an additional breakpoint between two existing ones. We have observed that when doing so, the two new regions should have the same maximum error (i.e.,

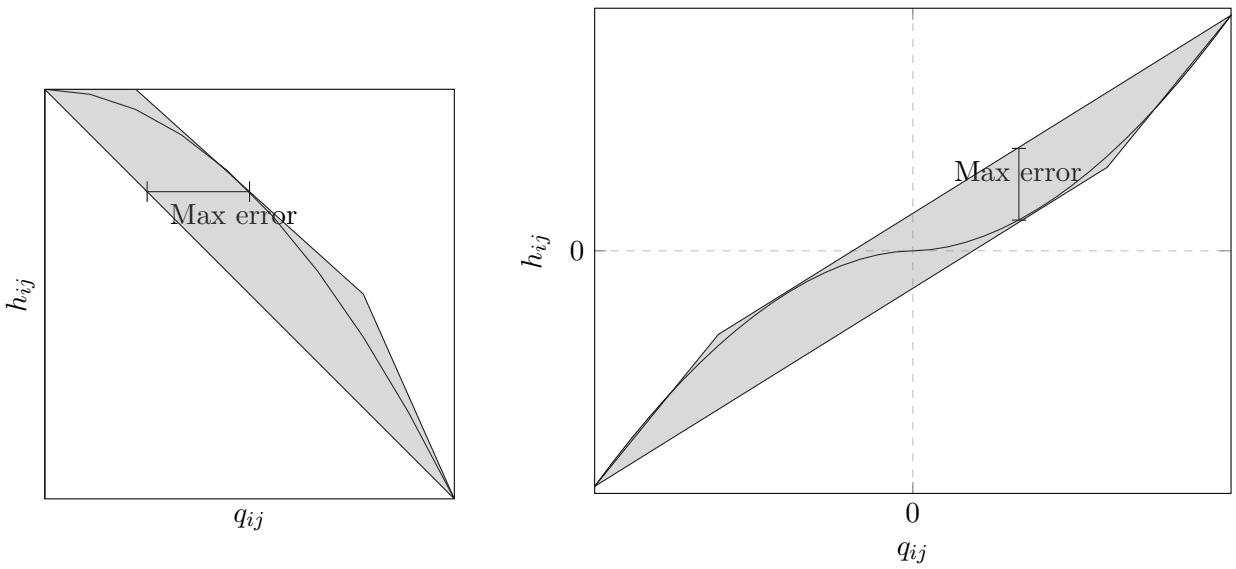

(a) Example of maximum errors for pump

(b) Example of maximum errors for HW curves

Figure 3: Examples of maximum errors for arcs

be symmetric) in order to efficiently use the newly introduced binary variables. This is depicted in Figure 4.

3.2 Computing the actual cost of a relaxed solution

From the procedure described in Section 3.1 one determines the maximum allowed error and thus computes the number of breakpoints (and binary variables) used to linearize pump curves and HW conditions. This model is then solved by means of a commercial MIP solver, and two situations may occur. First, if no solution exists to the linearized model, then the original model is also infeasible. If a solution to the linearized model exists, then it must be further examined to ensure it respects all constraints and conditions of the original model. This is done as follows and the overall procedure is described in Algorithm 1.

The solution is first tested on the EPANET simulator of water movement. If this solution is feasible and the cost obtained from EPANET is within a given error of the one obtained from the optimization phase, the solution is deemed feasible and is accepted, ending the optimization phase. Otherwise, if the solution cost from EPANET differs from that of the optimization, or if it is not feasible, we first try to repair the solution. If this is not successful, new tighter error bounds are computed and the

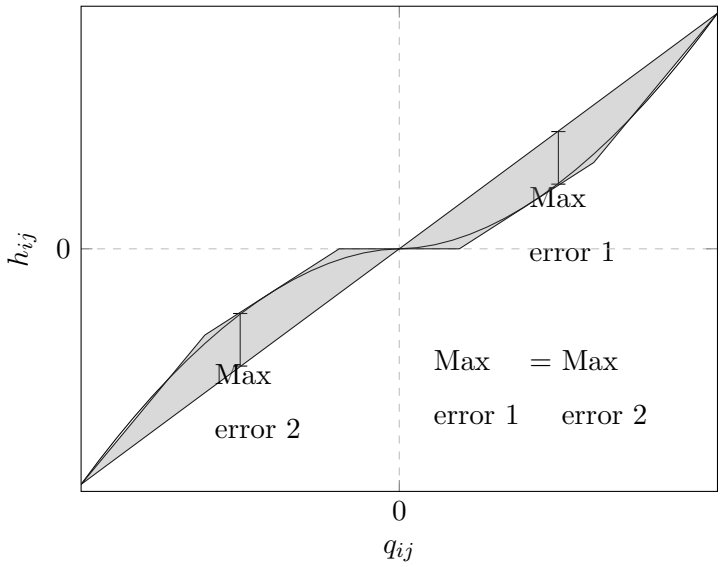

Figure 4: Example maximum error for a HW curve with three breakpoints

process is reiterated. We now describe how we repair a solution that does not respect all constraints of the problem.

We first check all pressure values, which cannot be negative for any nodes with demand. We describe in Algorithm 2 how we try to increase the initial volume of the water tanks and switching on pumps that are close to the node with an irregular pressure value. This is done in periods prior to the moment when the irregular pressure occurs, with preference to time periods with cheaper energy tariffs. If these steps are not sufficient to fix the pressure values, a new tighter error is computed and the process is reiterated.

Moreover, after pressure checks, the volume of water within the water tanks must be at least equal to that at the initial state. In Algorithm 3 we describe the procedure used to match the volume of water within the tanks. This is done by setting the initial values to those obtained at the end of the planning horizon. If this yields irregular pressure at nodes with demands, Algorithm 2 is applied. If the problem is now feasible, the solution is accepted. Otherwise, new tighter errors must be determined and the process is reiterated.

4 Computational experiments

In this section we describe the computational experiments carried out to evaluate the performance of our algorithm. All formulations were implemented using GAMS and solved with CPLEX version

Algorithm 1: Strategy to compute feasible solutions from the MIP relaxations

Input: A solution of Problem P.

Output: Optimal solution if the relaxed solution leads to a valid solution in the EPANET with a relative difference between the MIP objective function and the EPANET simulated cost less than a threshold. Otherwise infeasibility is reported.

```
Establish an initial maximum error ε for all pipes;
Compute relaxation Π^0 of P defining the number of breakpoints ensuring maximum error ε;
Solve relaxed model;
while relaxed model has an optimal solution q^i_opt do
    emulate solution on EPANET;
    if q^i_opt is a valid solution in EPANET then
        if emulated cost is within threshold to the relaxed MIP cost then
            return q^i_opt
        else
            construct Π^{i+1} reducing the maximum error for all pipes
        end
    else
        if irregular pressure values exist then
            go to Algorithm 2;
        else if final volume of tanks is lower than initial ones then
            go to Algorithm 3;
        else
            construct Π^{i+1} reducing the maximum error for all pipes
        end
    end
end
return "P is infeasible"
```

Algorithm 2: Irregular pressures correction

Input: A solution with irregular pressures

Output: A solution with regular pressures, or an indication to reformulate the problem

```
1  repeat
2      if tank closest to a node with irregular pressure starts at maximum capacity then
3          if there are switches after the moment of the last occurrence of irregular pressures then
4              advance a future switch for a period prior to the occurrence of irregular pressure
5          else
6              switch (on/off) available pump close to referred node before irregular pressures
                occur
7          end
8      else
9          increase the initial volume of tank by a predetermined amount
10     end
11     Emulate solution on EPANET;
12 until maximum number of iterations achieved or regular pressure values obtained;
13 if maximum number of iterations is reached then
14     go to line 10 of Algorithm 1
15 else
16     return "Current solution";
17     Continue from Algorithm 1;
18 end
```

Algorithm 3: Correction of the volume of water within tanks

Input: A solution with final tank levels lower than initial ones

Output: A solution in which initial and final levels respect constraints, or an indication to reformulate the problem

```
1  repeat
2      set initial levels of tanks equal to final ones;
3      repeat
4          emulate solution on EPANET;
5          if irregular pressure exists then
6              switch on the nearest pump available to the tank for which final level is lower than
                initial one, in the cheapest period
7          else
8              keep the current solution
9          end
10     until maximum number of iterations achieved or corrected water levels obtained;
11     if maximum number of iterations achieved then
12         go to line 10 of Algorithm 1
13     else
14         keep the current solution
15     end
16 until maximum number of iterations achieved or corrected water levels obtained;
17 if maximum number of iterations achieved then
18     go to line 10 of Algorithm 1
19 else
20     go to line 6 of Algorithm 1
21 end
```

12.6.3. All computations were executed on machines equipped with a Intel(R) Xeon(R) CPU E5-2698 processor running at 2.3GHz and 4 GB of memory. In the following, Section 4.1 provides a description of existing and new instances used in this research. In Section 4.2 we present the results of our experiments and our analysis.

4.1 Instances description

We have gathered instances available from the literature and introduce a new large one in this study. A small size instance used by Van Zyl et al. [26] contains two consuming nodes and one source with two parallel pumps. A booster pump and two water tanks complete the network for a total of 16 nodes and 18 arcs. Its schematic representation is depicted in Figure 5 and we will refer to it as Mini.

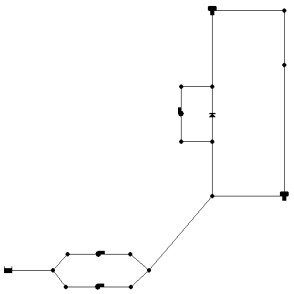

Figure 5: Mini network

A medium size instance is depicted in Figure 6 and is refereed to as Richmond Skeleton. It was used by Van Zyl et al. [26] and Giacomello et al. [14] and contains 48 nodes with six tanks and one source, and 51 arcs including seven pumps and one valve.

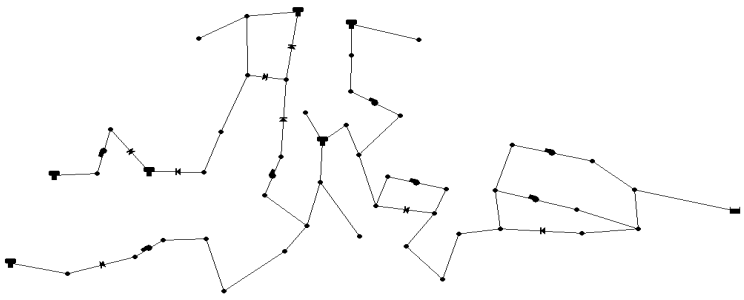

Figure 6: Richmond Skeleton network

The largest instance available in the literature is the Richmond Standard one, introduced by Van Zyl [25]. This network contains 872 nodes including six tanks and one reservoir, and 957 arcs including seven pumps and 21 valves. This network is depicted in Figure 7.

Figure 7: Richmond Stardard network

Table 1 presents the best results available in the literature for these three existing networks.

Network	Best results	Time (s)
Richmond Standard	£33,683.3 / yr (8,000 evaluations) [18]	8862
Richmond Standard	£32,581.4 / yr (50,000 evaluations) [18]	
Richmond Skeleton	£118.58 [14]	23
Mini	£312 [19]	N/A

Table 1: Best literature results

We introduce a new real instance from the city of Florianópolis, southern Brazil. This network serves a population of about 80,000 people with approximately 600,000 m^3 of water per month. The Florianópolis network consists of 654 arcs, seven of which are pumps and four valves, and 630 nodes including 560 consumer points, four tanks. We depict this new network in Figure 8.

This newly introduced network has a different energy pricing scheme, in four different levels as follows:

1. monomial: in this type of energy tariff, the user pays for the amount of energy consumed.

2. conventional: a maximum energy consumption is established on a contract, and no pump should exceed this usage at any point in time. In this case, the price of energy consumed does not vary throughout the day.

3. green hourly seasonal: a maximum energy consumption is established on a contract, as in the previous case, but energy consumption prices vary throughout the day.

4. blue hourly seasonal: here two maximum energy consumption levels exist: one for peak hours (between 18:00 and 21:00) and one for off-peak hours.

Figure 8: New real case of Florianópolis network

In Florianópolis, one pump operates in a blue hourly seasonal scheme, two in the green scheme, two in the conventional pricing, and two in the monomial pricing scheme. The real data obtained from the utility provider indicates that they incur a monthly cost of $75,216. This network and associated data can be made available upon request.

4.2 Computational results

We now present the results of computational experiments performed to evaluate the performance of our algorithms, and to compare the solutions obtained with those from the literature.

We start with the Mini network. We observe that it is defined with 15 arcs, but our preprocessing identified 10 short-cuts reducing this number to only five. No notable flows exist in this network. We first established a maximum error value of 0.96 meters for all pipes. This yields a model with 1392 binary variables. The average error for the pipes was computed at only 0.47 m.

Analyzing the results, we observed that for this case, the limitation of switching the pumps on and off does not seem to have contributed to the speed of convergence, nor did it influence the achieved value of the objective function. We noted that most of the time, the objective function of the model without limiting the number of switches was lower than in other instances (Figure 9). Indeed, for this case, at the end of 8 hours all instances converged to the same value (Table 2), which suggests that

the limitation of switching the pump on and off does not exclude the best primal solutions.

Maximum switches	Time (s)	Optimization solution	Lower bound	Gap (%)	EPANET simulation	Final gap (%)
2	28000	309.57	302.26	2.36	306.94	1.52
3	28800	309.57	300.54	2.92	306.94	2.08
4	28800	309.57	298.03	3.73	306.94	2.90
5	28800	309.57	300.49	2.93	306.94	2.10
∞	28800	309.57	301.07	2.75	306.94	1.91

Table 2: Solutions for the Mini network

For this network, we improved the solution from the literature [19] to 306.94, reducing it by 1.62%. The time to reach the best solution was 7 hours and 22 minutes. It is worth noting that we allow our method to change the initial volumes of the tanks, as long as their final levels are larger than the initial ones.

For the Richmond Skeleton network we set a maximum tolerated error value of 4.91 m for all pipes. With this maximum error, the problem was modeled using 1584 binary variables. We identified four arcs with notable flows and we define 11 arcs with short cuts, which reduced the number of arcs in which the head losses had to be defined from 44 to 33. After solving it, the mean maximum error of the pipes was only 1.04 m.

The results of our experiments are presented in Table 3 and Figure 10 and show that setting the maximum number of switches to 5 converged faster and yielded the best results.

Maximum switches	Time (s)	Optimization solution	Lower bound	Gap (%)	EPANET simulation	Final gap (%)
2	28800	111.20	57.59	48.21	114.42	47.67
3	28800	109.34	67.01	38.71	109.86	39.00
4	28800	106.42	81.71	23.21	114.64	28.72
5	28800	105.42	77.78	26.21	105.75	26.45
∞	28800	105.44	81.97	22.26	105.75	22.49

Table 3: Solutions for the Richmond Skeleton network

Again, our method improved the solutions from the literature. Our best solution improved that of

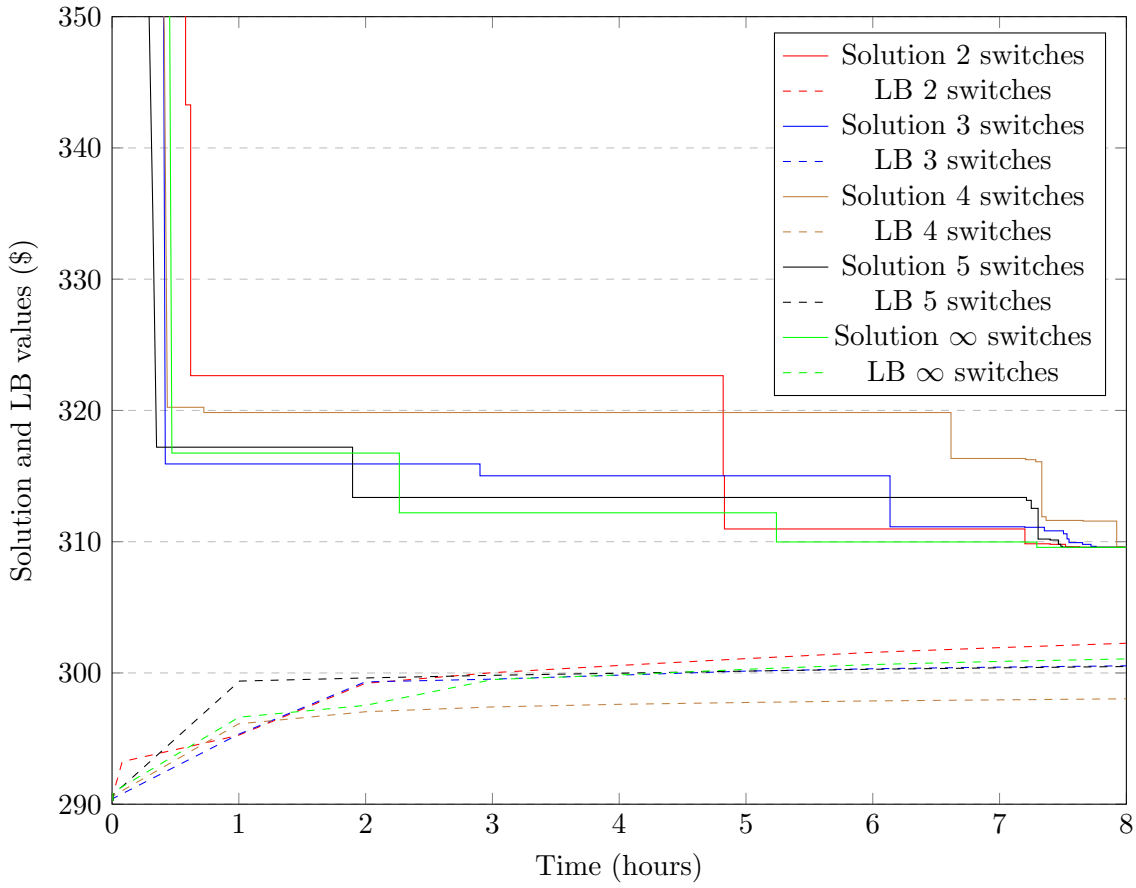

Figure 9: Evolution of the solutions over time for the Mini network

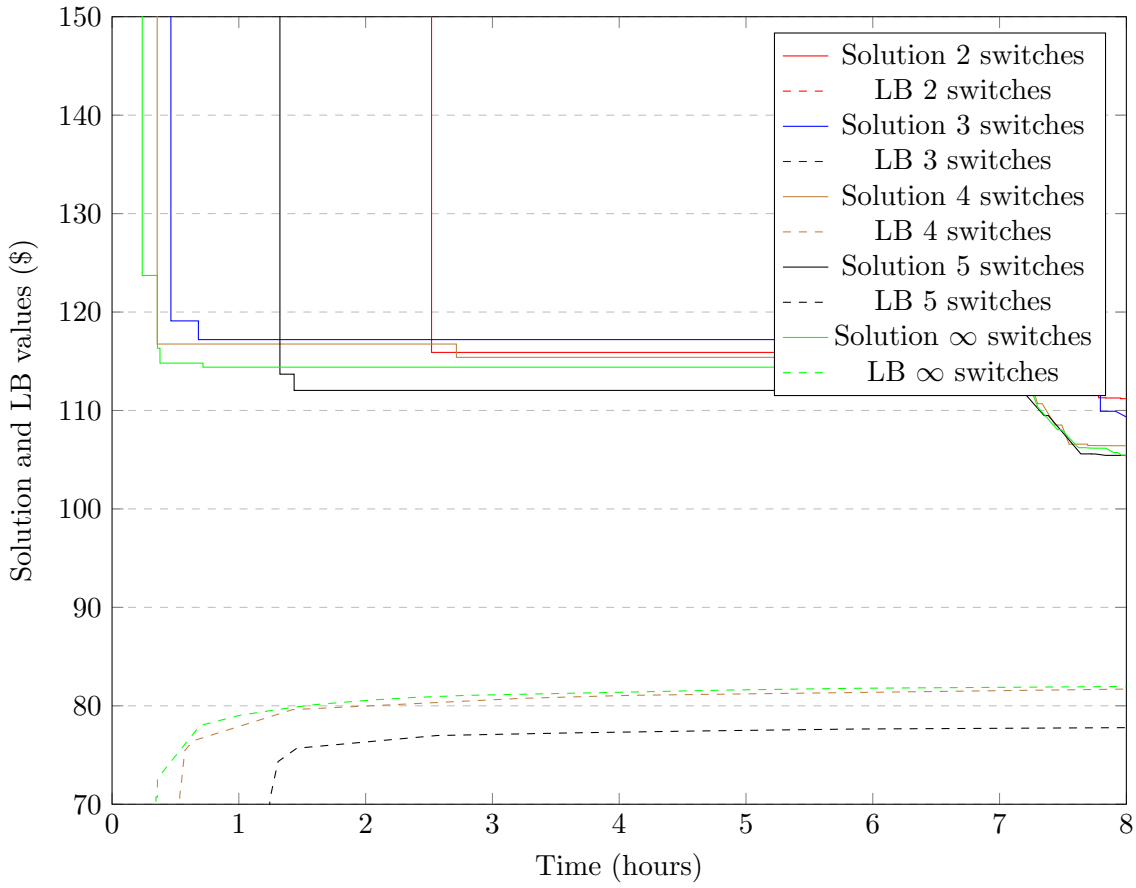

Figure 10: Evolution of the solutions over time for the Richmond Skeleton network

Giacomello et al. [14] by 10.82%. This type of problem can be solved over several hours, making our solution method usable in practice, as long as the utility provider has the solution on time to use it and save on operational costs.

For the last network from the literature, the Richmond Standard network, we defined a maximum error value of 17.07 m in height as maximum error for all pipes. Thereby, initially the problem was modeled with 1440 binary variables. As a simplification, we defined 190 arcs with notable flow and 122 short-cuts. After solving the problem, the mean maximum error of the pipes was only 0.37 m. We provided a known poor initial solution for the model and got the best result in the instance with 3 switches, in which we had a daily cost of \$88.80, (including switches costs). This solution had to go through proposed adjustments in Algorithms 2 and 3 resulting in a cost of \$ 86.41 in the EPANET simulator (excluding switches costs).

The best result of the literature we found for this network is presented in López-Ibáñez et al. [18] where the authors obtained an annual cost of \$ 32,581.4, resulting in a daily cost of \$89.26. They did not report accounting for switching costs, although they limited their quantity. Thus, for this network, our method improved the best literature solution by 3.20%. We also emphasize that for the instance with 3 switches, after 2 and a half hours the objective function had already reached a solution of \$90.03, a value very close to the value found after 8 hours (see Figure 11).

Max. Switches	Time (s)	Optimization Solution[1]	Lower bound	Gap (%)	EPANET Simulation[2]	Final gap (%)
2	28800	94.99	67.66	28.77	100.98	32.99
3	28800	88.80	68.42	22.94	86.41	20.82
4	28800	99.89	68.50	31.42	97.66	29.85
5	28800	95.91	68.44	28.64	102.60	33.29
∞	28800	95.69	68.60	28.31	102.60	33.13

[1]Includes cost of switches. [2]Does not include cost of switches.

Table 4: Solutions for the Richmond Standard network

The Florianópolis network requires further modeling efforts to account for its non-standard energy consumption rates. This is now presented in Section 4.2.1 followed by the computational results for this network in Section 4.2.2.

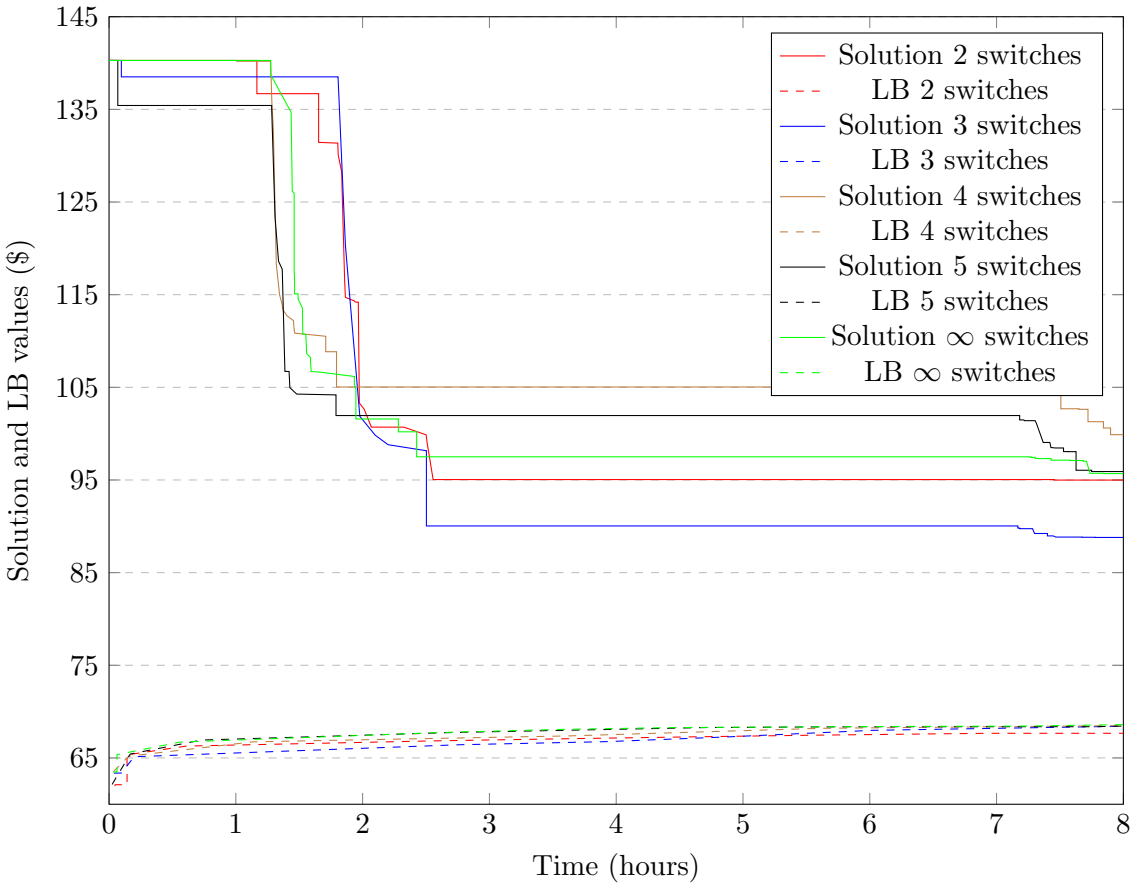

Figure 11: Evolution of the solutions over time for Richmond Standard network

4.2.1 Modeling non-standard energy consumption

To represent the new energy rates, we define the following new sets:

- $\mathcal{P}^A \subset \mathcal{P}$: subset of pipes containing pumps subject to the blue hourly seasonal rate
- $\mathcal{P}^V \subset \mathcal{P}$: subset of pipes containing pumps subject to the green hourly seasonal rate
- $\mathcal{P}^C \subset \mathcal{P}$: subset of pipes containing pumps subject to the conventional rate
- $\mathcal{T}^P \subset \mathcal{T}$: subset of periods containing peak times,

and the following parameters:

- C_{ij}^{DaP}: electricity cost during the peak hours of the blue hourly seasonal rate of pump (i, j) (in monetary units/kW)
- C_{ij}^{DaFP}: electricity cost during out-of-peak hours of blue hourly seasonal rate of pump (i, j) (in monetary units/kW)
- C_{ij}^{DV}: electricity cost during the green hourly seasonal rate of pump (i, j) (in monetary units/kW)
- C_{ij}^{DC}: electricity cost of the conventional rate for pump (i, j) (in monetary units/kW)
- M: number of periods (days) which will be optimized
- $W_{oij}^P(Q_{oij}^P)$: amount of kW consumed by pump P in the flow point Q_{oij}^P, where: $W_{oij}^P(Q_{oij}^P) = \frac{\gamma Q_{o,ij}^P H_{o,ij}^P}{10^6 \eta_{ij}} \Leftrightarrow \frac{Z_{o,ij}^P}{C_{ijt}}$.

Finally, we define the following new variables:

- a_{ij}^P: contracted demand for peak times, for pump (i, j) subject to the blue hourly seasonal rate (in kW)
- a_{ij}^{FP}: contracted demand for out-of-peak times, for pump $i, j)$ subject to the blue hourly seasonal rate (in kW)
- v_{ij}: contracted demand for pump (i, j) subject to the green hourly seasonal rate (in kW)
- c_{ij}: contracted demand for pump (i, j) subject to the conventional rate (in kW).

Thus, the objective function (24) must be replaced by (41)–(45):

$$min \sum_{t\in\mathcal{T}} \sum_{ij\in\mathcal{P}} \sum_{o\in\mathcal{O}} \lambda_{o,ij,t} Z^P_{o,ij} + \frac{\left(\sum_{ij\in\mathcal{P}^A} C^{DaFP}_{ij} a^{FP}_{ij} + \sum_{ij\in\mathcal{P}^A} C^{DaP}_{ij} a^{P}_{ij} + \sum_{ij\in\mathcal{P}^V} C^{DV}_{ij} v_{ij} + \sum_{ij\in\mathcal{P}^C} C^{DC}_{ij} c_{ij}\right)}{M} \tag{41}$$

$$\sum_{o\in\mathcal{O}} \lambda_{o,ij,t} W^P_{o,ij} \leq a^P_{ij} \quad \forall (i,j) \in \mathcal{P}^A, \forall t \in \mathcal{T}^P \tag{42}$$

$$\sum_{o\in\mathcal{O}} \lambda_{o,ij,t} W^P_{o,ij} \leq a^{FP}_{ij} \quad \forall (i,j) \in \mathcal{P}^A, \forall t \in \mathcal{T} \backslash \mathcal{T}^P \tag{43}$$

$$\sum_{o\in\mathcal{O}} \lambda_{o,ij,t} W^P_{o,ij} \leq v_{ij} \quad \forall (i,j) \in \mathcal{P}^V, \forall t \in \mathcal{T} \tag{44}$$

$$\sum_{o\in\mathcal{O}} \lambda_{o,ij,t} W^P_{o,ij} \leq c_{ij} \quad \forall (i,j) \in \mathcal{P}^C, \forall t \in \mathcal{T}. \tag{45}$$

4.2.2 Computational results for the new Florianópolis network

We have arbitrated a maximum error of 10 m for all pipes. Using this value, most pipes could be modeled with only one feasible region in the relaxed model, resulting in very few binary variables. The mean maximum error of the pipes was then 1.24 m. Out of the 654 arcs whose flow variables would have to be computed, we determined 233 arcs with a predefined flow, reducing the number of flow variables to 421, which represented a reduction of approximately 35% in the number of variables. In addition, another 13 arcs were identified as shortcuts and had their head loss set to zero.

Since there is no benchmark for this instance, we have first analyzed the effects of simplifications presented in Section 2.3. These are compared on the basis of the convergence of the models, without any limitation on the number of switches of the pumps. We present the evolution of the solution quality in Figure 12, and in Table 5 we present the final results of the model and the EPANET simulation.

Maximum switches	Time (s)	Optimization solution	Lower bound	Gap (%)	EPANET simulation	Final Gap (%)
∞	28800	1709.4	1367.3	20.0%	2085.5	34.4%

Table 5: Solution for the Florianópolis network

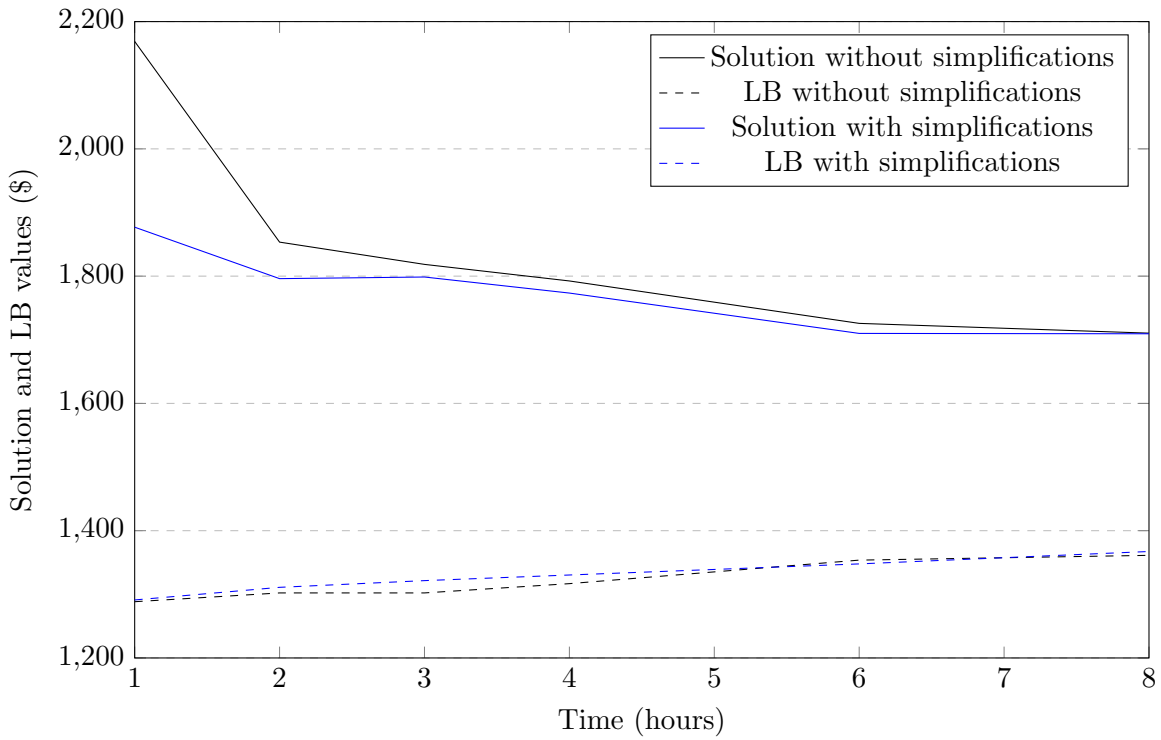

Figure 12: Comparison of the evolution of solutions with and without simplifications

Analyzing the results of the optimization phase, we observe that the model with simplifications started from a significantly better solution, but that both versions of the model converged to the same solution at the end of the optimization phase. Regarding the evolution of the lower bounds, the results were similar over the time, and at the end of the 8 hours of computing time, the lower bound of the non-simplified model was higher, indicating that at that point, no solution was lost from simplifying the model.

The best solution resulted in a cost of $1709 and was emulated in EPANET, yielding a solution cost of $1905, but with irregular pressure values. After applying our corrective algorithms, we reached a feasible value of $2085.48, which is 16.82% lower than the solution used by the water service provider. These results are presented in Table 6.

We have also observed that not only the energy cost was lower, but also the energy consumption decreased. This means that our solution is not using more energy from cheap tariffs, but is decreasing energy consumption overall. For the optimized solution, the pumps required a total of 7481 kW, against 8995 kW for the solution in used by the utility provider, representing a reduction of 16.83%. It can be seen that the percentage reduction obtained in energy consumption (16.83% in kW) was

	Math model ($)	EPANET solution ($)	EPANET after corrections ($)	Service provider ($)	Difference ($)	Difference (%)
Consumption	1550.03	1730.26	1906.57	2068.93	162.36	7.84
Demand	159.40	175.52	178.91	438.28	259.37	59.17
Total	1709.43	1905.78*	2085.48**	2507.21	421.73	16.82
Lower bound	1367.30					

*Infeasible solution

*Feasible solution

Table 6: Details of the Florianópolis network solution

higher than the reduction of costs related to consumption (7.84% in $). This is a very positive outcome of this method, and could lead to further analysis and optimization.

The reduction of the energy supplied is also due to the fact that the total energy lost by friction in the pipes has been lower in the optimized solution. The value decreased from 2958 kW lost by friction in the solution of the provider, to 2146 kW in the optimized solution. Table 7 summarizes the differences in energy consumption in the two scenarios.

	Proposed solution (kW)	Service provider (kW)	Difference (kW)	Difference (%)
Power supply	7481	8995	1514	16.83
Losses	2146	2958	812	27.45
Relative losses	28.69%	32.88%		

Table 7: Comparison between the optimized and the service provider solutions

We deduce that the difference between the energy use between the optimized solution and the service provider ones does not derive solely from the reduction of losses. For this difference of 1514 kW of energy consumed, only 812 kW (53.63%) are explained by the reduction of losses by friction. We assume that the remaining savings come from the increased use of the most efficient pumps in the system and the reduction of usage of less efficient pumps; moreover, our solution makes better use of reservoirs, as it is known that working with reservoirs at different levels changes the amount of energy consumed by the pumps.

In addition, another reason for lower losses in our solution may come from use of the most central

pumps in the system, since these are closer, on average, to the demand points. These results show that the use of the optimization tool in the WDS operation is not only able to reduce the cost with energy, but also to reduce the energy consumption itself, which represents an environmental benefit of its use.

The proposed gains obtained in this research are compatible with those of other applications found in the literature, such as the city of Valencia (Spain) [20], and in Haifa (Israel) [23], where financial gains of 17.6% and 25% were reported, respectively.

5 Conclusions

In this paper we have proposed a new linear relaxation for a non-linear integer programming formulation for optimizing water distribution. In order to help in obtaining good solutions, new simplifications were presented in order to reduce the number of combinations of feasible solutions and significantly reducing the number of variables and constraints of the model. We have tested our methods in three benchmark instances from the literature, improving all previous results.

We have also introduced a new large network to the literature, based on the WDS of the city of Florianópolis, Brazil. Our method reduced the cost of the service provider by more than 16%, in addition to a reduction of 27.45% of the load losses. A side benefit of our solution is that not only costs have been reduced, but energy consumption has decreased by almost 17% as well. We have thus demonstrated that the optimization of the WDS operation can not only bring financial gains, but can also bring environmental benefits.

Future research can focus on improving the optimization method or on the side benefits of the cost optimization. New valid inequalities and simplifications could be developed, which would reduce the need for correction phases, which inevitably increases costs. Different works on reducing network complexity exist, such as those dealing with gas, electricity and water (see, e.g., Paluszczyszyn [21]). Moreover, the use of initial solutions based on previous knowledge of the system operation can significantly enhance its performance [14]. Finally, we have demonstrated that when optimizing for cost reductions, a side benefit we have observed is an overall reduction in energy consumption. From an environmental perspective, using fewer resources is more important than reducing a few percentage points in costs.

References

[1] L. Addams, G. Boccaletti, M. Kerlin, and M. Stuchtey. Charting our water future: Economic frameworks to inform decision-making. *McKinsey & Company, New York*, 2009.

[2] C. Bragalli, C. D'Ambrosio, J. Lee, A. Lodi, and P. Toth. On the optimal design of water distribution networks: a practical MINLP approach. *Optimization and Engineering*, 13(2):219–246, 2012.

[3] J. Burgschweiger, B. Gnädig, and M. C. Steinbach. Nonlinear programming techniques for operative planning in large drinking water networks. *Open Applied Mathematics Journal*, 3:14–28, 2009.

[4] B. Coelho and A. Andrade-Campos. Efficiency achievement in water supply systems: A review. *Renewable and Sustainable Energy Reviews*, 30:59–84, 2014.

[5] R. Connor. The United Nations world water development report 2015: Water for a sustainable world. Technical report, UNESCO Publishing, 2015.

[6] G. Cornuéjols. Valid inequalities for mixed integer linear programs. *Mathematical Programming*, 112(1):3–44, 2008.

[7] C. D'Ambrosio, A. Lodi, S. Wiese, and C. Bragalli. Mathematical programming techniques in water network optimization. *European Journal of Operational Research*, 243(3):774–788, 2015.

[8] G. B. Dantzig. On the significance of solving linear programming problems with some integer variables. *Econometrica, Journal of the Econometric Society*, 28(1):30–44, 1960.

[9] M. M. Eusuff and K. E. Lansey. Optimization of water distribution network design using the shuffled frog leaping algorithm. *Journal of Water Resources Planning and Management*, 129(3): 210–225, 2003.

[10] Z. W. Geem. Optimal cost design of water distribution networks using harmony search. *Engineering Optimization*, 38(03):259–277, 2006.

[11] B. Geiβler, A. Martin, A. Morsi, and L. Schewe. Using piecewise linear functions for solving MINLPs. In J. Lee and S. Leyffer, editors, *Mixed Integer Nonlinear Programming*, pages 287–314. Springer, Spring Street, New York, NY 10013, USA, 2012.

[12] B. Geiβler, A. Morsi, and L. Schewe. A new algorithm for MINLP applied to gas transport energy cost minimization. In M. Jünger and G. Reinelt, editors, *Facets of Combinatorial Optimization*, pages 321–353. Springer, Cologne, Germany, 2013.

[13] B. Ghaddar, J. Naoum-Sawaya, A. Kishimoto, N. Taheri, and B. Eck. A lagrangian decomposition approach for the pump scheduling problem in water networks. *European Journal of Operational Research*, 241(2):490–501, 2015.

[14] C. Giacomello, Z. Kapelan, and M. Nicolini. Fast hybrid optimization method for effective pump scheduling. *Journal of Water Resources Planning and Management*, 139(2):175–183, 2012.

[15] K. James, S. L. Campbell, and C. E. Godlobe. Watergy: Taking advantage of untapped energy and water efficiency opportunities in municipal water systems. Technical report, Alliance to Save Energy, 2002.

[16] F. Liu, A. Ouedraogo, S. Manghee, and A. Danilenko. A primer on energy efficiency for municipal water and wastewater utilities. Technical report, World Bank, 2012.

[17] M. López-Ibáñez, T. D. Prasad, and B. Paechter. Ant colony optimization for optimal control of pumps in water distribution networks. *Journal of Water Resources Planning and Management*, 134(4):337–346, 2008.

[18] M. López-Ibáñez, T. D. Prasad, and B. Paechter. Ant colony optimization for optimal control of pumps in water distribution networks. *Journal of Water Resources Planning and Management*, 134(4):337–346, 2008.

[19] A. Marchi, A. R. Simpson, and M. F. Lambert. Optimization of pump operation using rule-based controls in EPANET2: New ETTAR toolkit and correction of energy computation. *Journal of Water Resources Planning and Management*, 186:210–217, 2017.

[20] F. Martínez, V. Hernández, J. M. Alonso, Z. Rao, and S. Alvisi. Optimizing the operation of the Valencia water-distribution network. *Journal of Hydroinformatics*, 9(1):65–78, 2007.

[21] D. Paluszczyszyn. *Advanced modelling and simulation of water distribution systems with discontinuous control elements*. PhD thesis, De Montfort University, 2015.

[22] R. Rovatti, C. D'Ambrosio, A. Lodi, and S. Martello. Optimistic MILP modeling of non-linear optimization problems. *European Journal of Operational Research*, 239(1):32–45, 2014.

[23] E. Salomons, A. Goryashko, U. Shamir, Z. Rao, and S. Alvisi. Optimizing the operation of the Haifa-a water-distribution network. *Journal of Hydroinformatics*, 9(1):51–64, 2007.

[24] H. D. Sherali, S. Subramanian, and G. V. Loganathan. Effective relaxations and partitioning schemes for solving water distribution network design problems to global optimality. *Journal of Global Optimization*, 19(1):1–26, 2001.

[25] J. E. Van Zyl. *A methodology for improved operational optimization of water distribution systems*. PhD thesis, University of Exeter, 2001.

[26] J. E. Van Zyl, D. A. Savic, and G. A. Walters. Operational optimization of water distribution systems using a hybrid genetic algorithm. *Journal of Water Resources Planning and Management*, 130(2):160–170, 2004.

[27] D. Verleye and E.-H. Aghezzaf. Optimising production and distribution operations in large water supply networks: A piecewise linear optimisation approach. *International Journal of Production Research*, 51(23-24):7170–7189, 2013.

[28] Z. Y. Wu, P. Sage, and D. Turtle. Pressure-dependent leak detection model and its application to a district water system. *Journal of Water Resources Planning and Management*, 136(1):116–128, 2009.